Supporting Information

A Binder-free $NiCo_2O_4$ Nanosheets/3D Elastic N-Doped Hollow Carbon Nanotube Sponge Electrode with High Volumetric and Gravimetric Capacitance for Asymmetric Supercapacitor

Hao Tong,‡[*a] Shihong Yue,‡[a] Liang Lu,[a] Fengqiao Jin,[a] Qiwei Han,[b] Xiaogang Zhang,[*a] Jie Liu,*[b]

[a] Jiangsu Key Laboratory of Materials and Technology for Energy Conversion, College of Material Science and Engineering, Nanjing University of Aeronautics and Astronautics, Nanjing, 210016, China.

[b] Department of Chemistry, Duke University, Durham, North Carolina, 27708, USA.

*Corresponding authors. E-mail: tongh@nuaa.edu.cn;; azhangxg@nuaa.edu.cn; jliu@chem.duke.edu

‡ These authors contributed equally to this work.

Experimental Section

The synthesis of NSCS

The single-walled carbon nanotubes (CNTs) purchased from Shenzhen Nanotech Port Co. Ltd. were refluxed in nitric acid, and then extensively washed and diluted with deionized water, obtaining 1 mg mL^{-1}. A freshly washed PU sponge was then immersed into the dispersion to make the absorption of the CNTs into the sponge. After being dried, the PU sponge coated with CNTs was heated in a nitrogen atmosphere at 500 °C for 0.5 h with a heating rate of 5°C min^{-1}.

The synthesis of $NiCo_2O_4$ on NSCS

Synthesis $NiCo_2O_4$ nanosheets supported on NSCS: In a typical process, $NiCl_2 \cdot 6H_2O$, $CoCl_2 \cdot 6H_2O$ and urea were successively added into a mixture of deionized water and methanol with vigorous stirring forming homogeneous solution. Then the solution was transferred into a 40 mL Teflon-lined autoclave and a 1×1×1 cm^3 of NSCS was immersed, kept at 120 °C for 6h. After cooled down, taken out the sponge and washed with deionized water and anhydrous ethanol several times, then dried at 60 °C overnight, the sample was marked as NiCo-precursor/NSCS, then the sample was annealed at 300 °C for 2 h. Finally, the $NiCo_2O_4$/NSCS was obtained.

The flower-like $NiCo_2O_4$ powders was synthesized in the same method without the adding of NGN/CNTs film as a comparison sample. $NiCo_2O_4$/Carbon cloth and $NiCo_2O_4$/Ni foam were also synthesized in the same condition as $NiCo_2O_4$/NSCS.

The synthesis of NGN/CNTs flexible film:

Nitrogen-doped graphene (NGN)/CNTs film was synthesized *via* a same method by our group reported before. [1] The GO was prepared by a previous modified Hummers' method but with a slight modification from flake graphite. The activated GO as synthesized via an activated process by potassium permanganate e. After purification, the activated GO was

further dispersed to form homogeneous aqueous solution (2 mg mL^{-1}). Multiwalled carbon nanotube (95 % purity, 10-20 nm average diameter size, 100-160 g m^{-2}, ShenZhen Nanoport, LTD) was modified through a 70°C hot hydrothermal bath in 3M Nitric acid treating for 2 hours .After purification and dispersion, forming to the MWCNTs solution (1 mg mL^{-1}). The sodium dodecyl sulfate (SDS, 5 mg), MWCNTs aqueous (1.5 mL) and activated GO solution (22 mL) were mixed and stirred together for 0.5 h. Then the homogeneous mixture solution was filtered using a mixed cellulose ester filter membrane (0.22 um pore size) by vacuum filter. After freeze drying, then the film was transferred into 80 mL Teflon-lined autoclave with ammonium hydroxide and kept in 180 °C for 24 hours. The NGN/CNTs film was obtained.

Material Characterization

Scanning electron microscopy (FE-SEM, Hitachi S4800) and transmission electron microscopy (TEM, JEOL JEM-2100) were used to investigate the micro/nanoscale structure of the samples. The mechanical properties was carried out by Instron 5967. The crystal structures were measured through X-ray diffraction (XRD) by a Bruker D8 Advanced X-ray diffractometer with Cu Kα radiation (0.15406 nm). Raman spectra were measured on a HORIBA Scientific LabRAM HR Raman spectrometer system using a 532.4 nm laser. X-ray photoelectron spectroscopy (XPS) measurements were performed using a PHI 550 spectrometer with Al-K_α (1486.6 eV) as the X-ray source.

Electrochemical measurement:

All electrochemical measurements were carried out using a two electrode or three electrode system in 6 M KOH electrolyte at room temperature. The as-prepared $NiCo_2O_4$/NSCS (1 cm ×1 cm×0.5 cm) was pressed under pressure and served as the working electrode, a platinum foil and a saturated calomel electrode (SCE) were used as counter

electrode and reference electrode respectively in a three electrode system. The $NiCo_2O_4$/NSCS and NGO/CNTs were directly served respectively as the flexible positive and negative electrodes for asymmetric supercapacitors. The mass ratio of positive to negative electrode was 0.563 being decided by the charge balance relationship of $q+ = q-$ and based on the equation (1). The cyclic voltammetry (CV), galvanostatic charge/discharge (GCD) and electrochemical impedance spectroscopy (EIS) measurements were carried out with a CHI 660B electrochemical working station.

$$m^- = m^+ \times (C^+ \times \Delta V^+)/(C^- \times \Delta V^-) \quad (1)$$

In the three-electrode system, the specific gravimetric capacitance(C_g, F g^{-1}) of the electrodes can be calculated by the following equation:

$$C_g = \frac{I\Delta t}{m\Delta V} \quad (2)$$

Where C_g (F g^{-1}) is the gravimetric capacitance, I (A) is the discharge current, Δt (s) refers to the time for a full discharge, m (g) is the mass of active material (or the total electrode), and ΔV (V) is the potential window of a full discharge.

The specific volumetric capacitance (C_v, F cm^{-3}) of the electrodes can be calculated *via* the following equation:

$$C_v = C_g \rho \quad (3)$$

$$\rho = \frac{m}{Vol} \quad (4)$$

Where C_v (F cm^{-3}) is the volumetric capacitance, *Vol* represents the volume of the whole electrode materials, ρ is the mass density of active material.

The asymmetric supercapacitor (ASC) was fabricated and measured in a two-electrode system. The specific gravimetric capacitance (C_g, F g^{-1}) and volumetric capacitance (C_v, F cm^{-3}) of the ASC was calculated based on the following equation:

$$C_g = \left(\int IdV\right)/(vMV) \quad (5)$$

$$C_v = C_g \rho \quad (6)$$

$$\rho = \frac{M}{VOL} \quad (7)$$

Where C_g (F g^{-1}) is the gravimetric capacitance, C_v (F cm^{-3}) is the volumetric capacitance, I (A) is the current, v is the potential scan rate (mV s^{-1}), M (g) represents the total mass of active material (or the whole mass) in two electrodes, VOL (cm^{-3}) represents the total volume of two electrodes, ρ is the mass density and V (V) is the potential window of the ASC.

The energy density E (E_g, E_v; W h kg^{-1}, W h L^{-1}) and power density P (W kg^{-1}, W L^{-1}) of the device could be calculated as follow equation:

$$E_g = \frac{C_g V^2}{2} \quad (8)$$

$$E_V = E_g \rho \quad (9)$$

$$P = \frac{E}{\Delta t} \quad (10)$$

Where V (V) is the potential window of the ASC, Δt (s) is the time for a sweep segment.

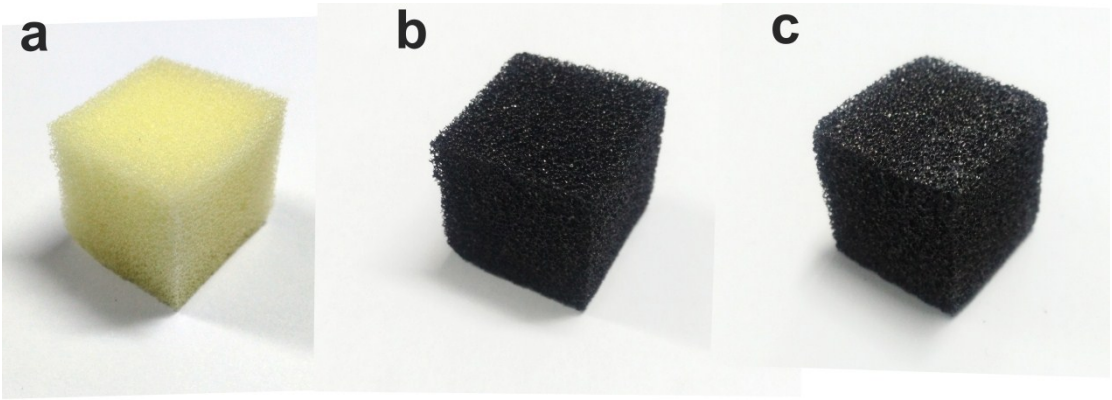

Fig. S1 (a) PU foam, (b) CNTS/PU sponge and (c)NSCS

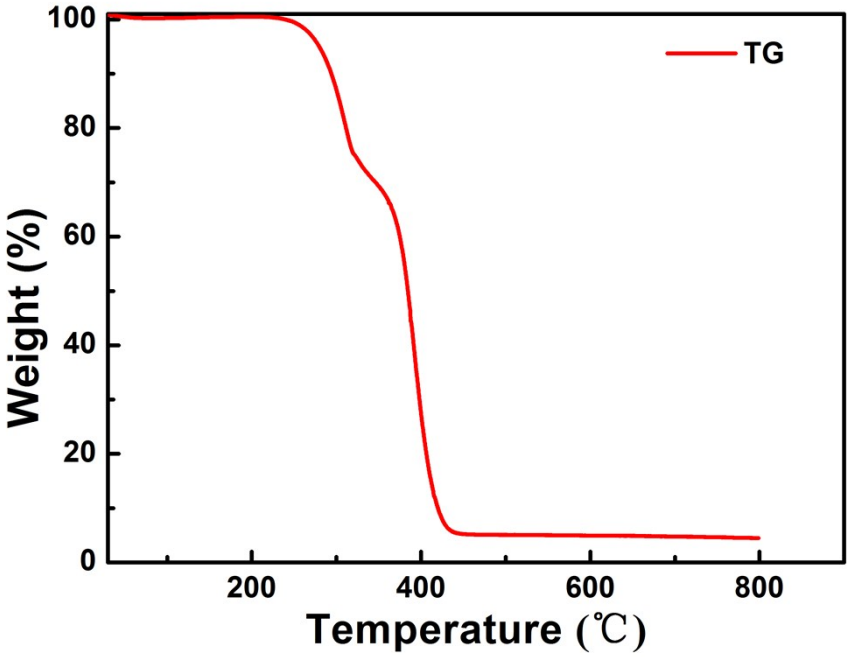

Fig. S2 TGA curve of PU sponge template.

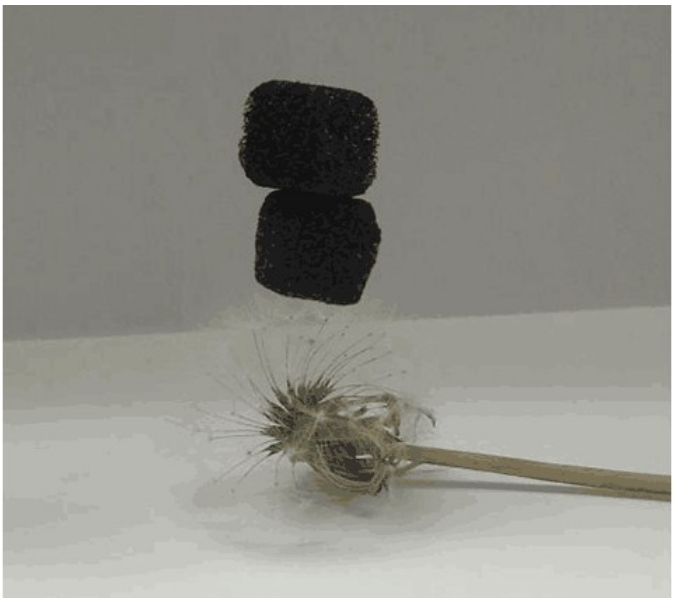

Fig. S3 The ultra-light NSCS on dandelion.

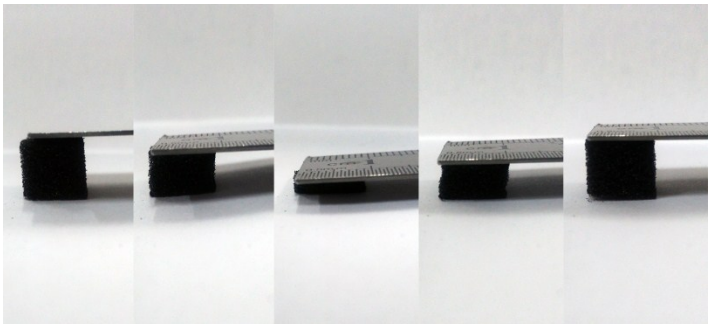

Fig. S4 Compression and recover process of NSCS.

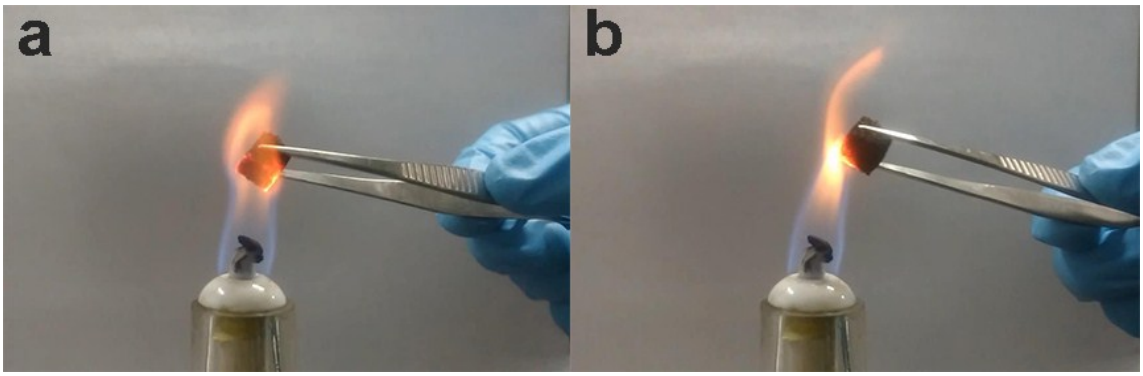

Fig. S5 NSCS in ethanol flame

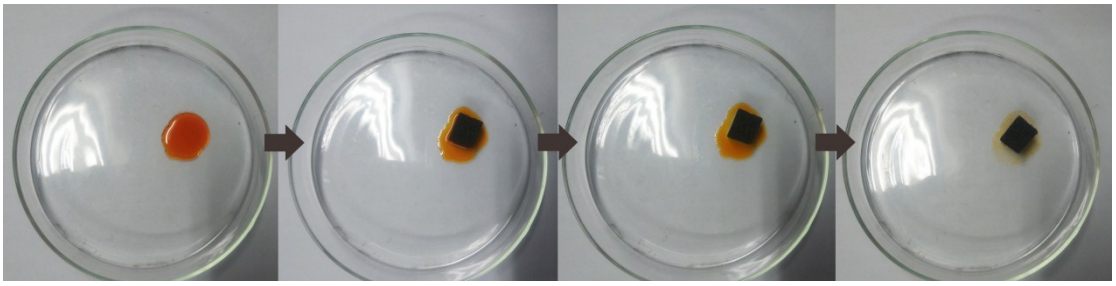

Fig. S6 Active absorption of oil by a small NSCS.

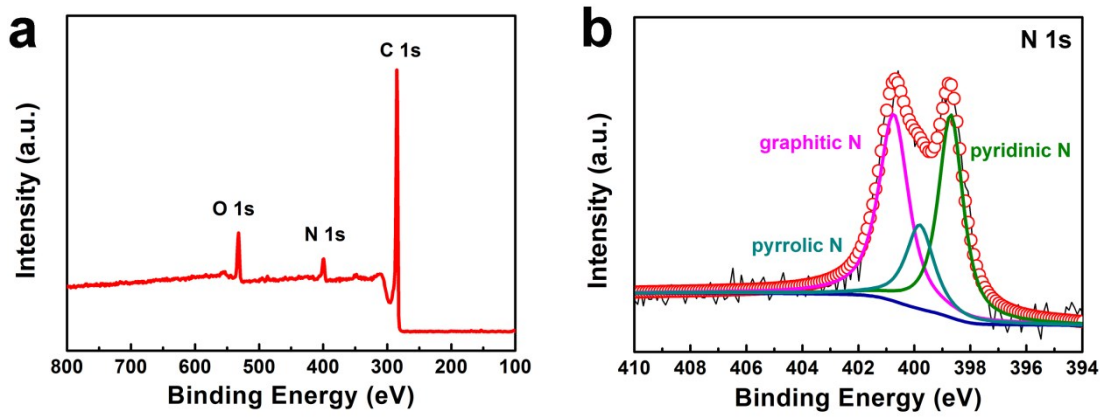

Fig. S7 XPS results: (a) survey and (b) N 1s for NSCS

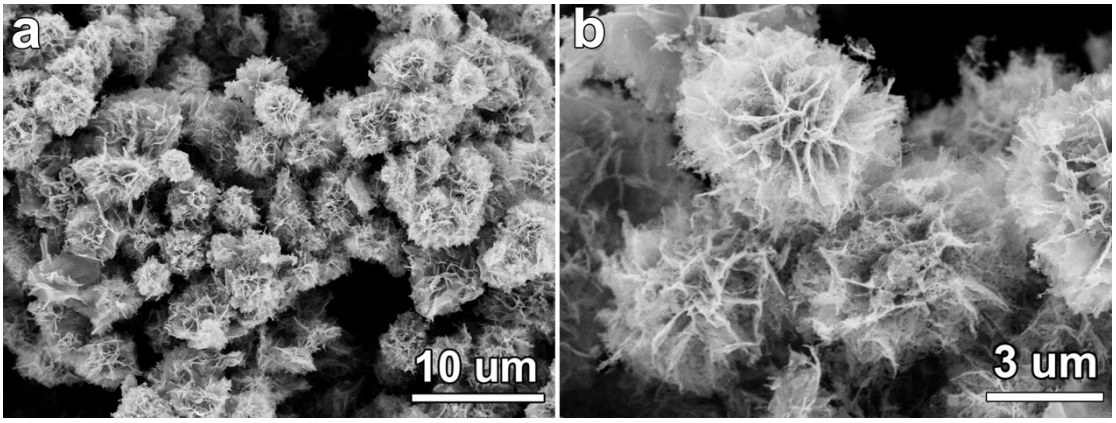

Fig. S8 SEM images of $NiCo_2O_4$ powder.

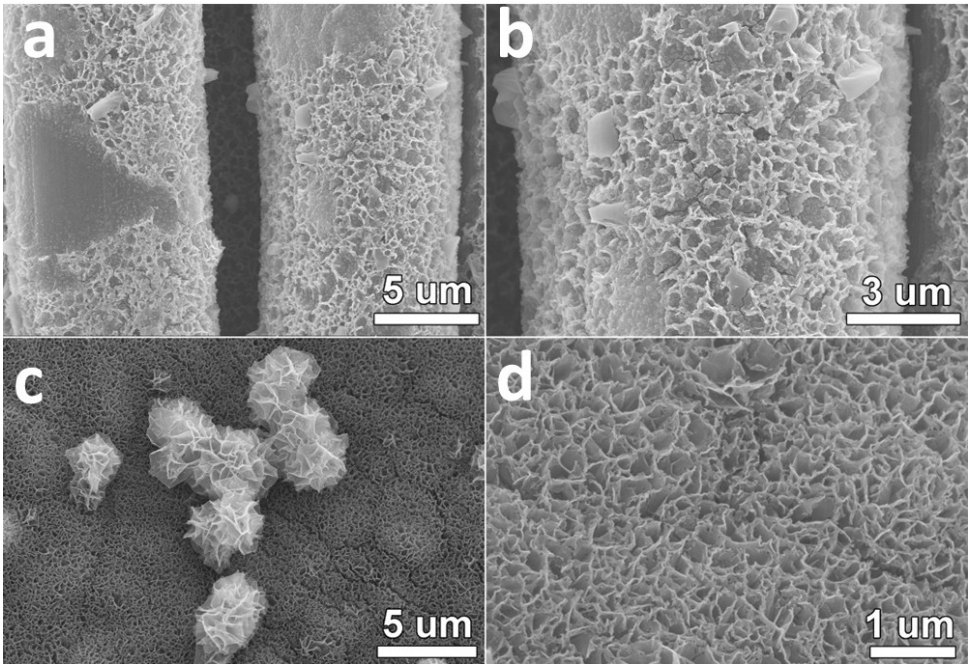

Fig.S9 SEM images of $NiCo_2O_4$/Carbon fiber (a and b) and $NiCo_2O_4$/Ni foam(c and d).

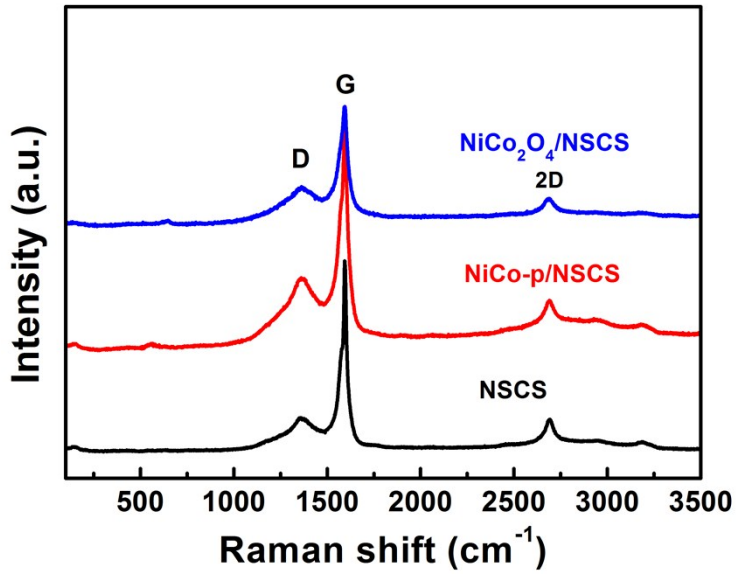

Fig. S10 Raman spectroscopy of NSCS, NiCo-p/NSCS and $NiCo_2O_4$/NSCS

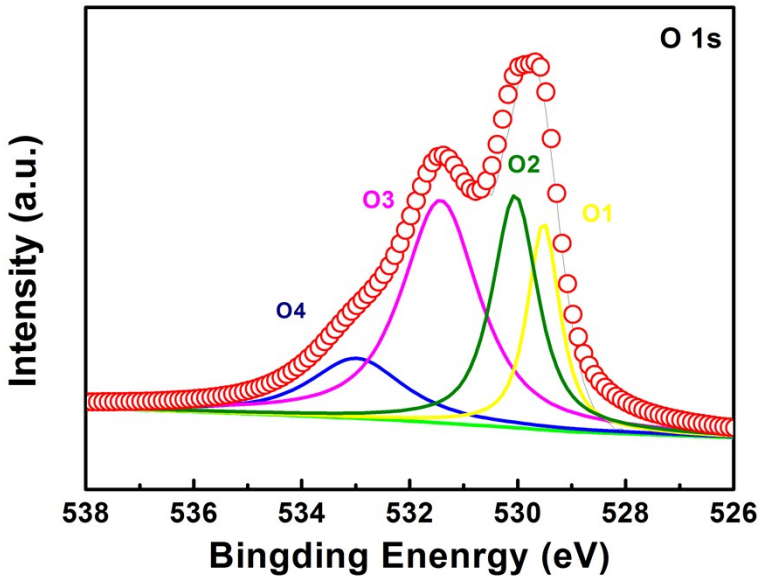

Fig. S11 XPS results of O 1s for $NiCo_2O_4$/NSCS

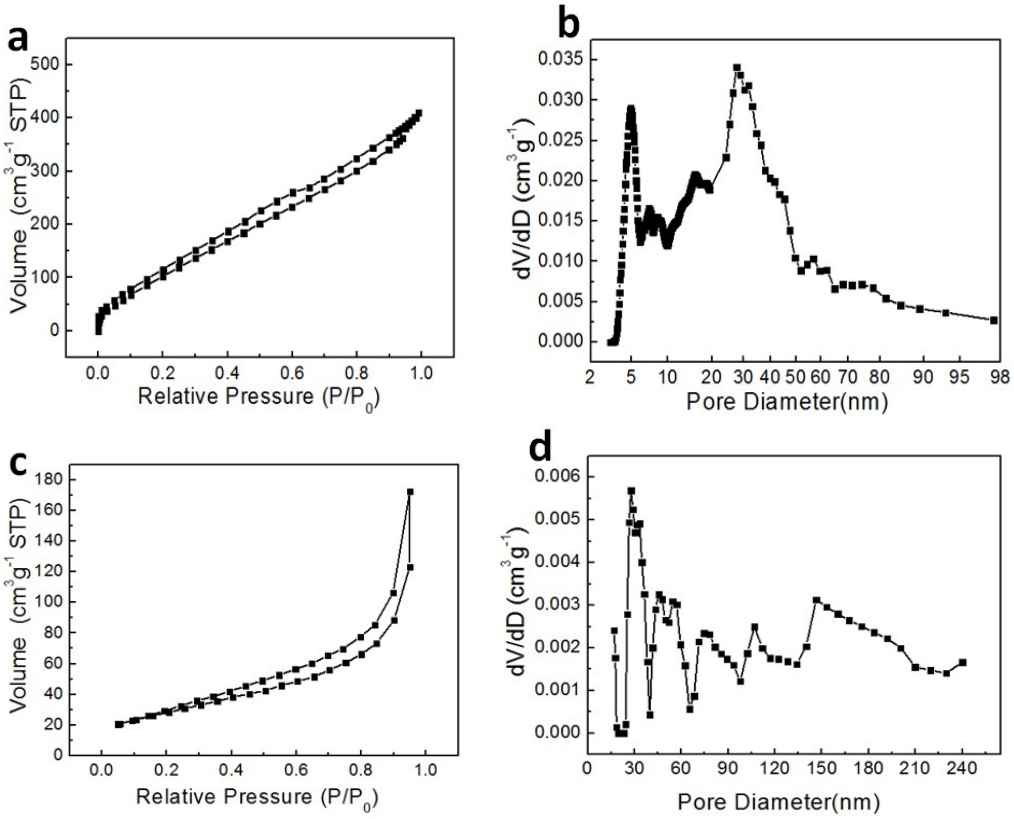

Fig. S12 (a) N_2 adsorption–desorption isotherms of NSCS, (b) the pore size distribution of NSCS,(c) N_2 adsorption–desorption isotherms of $NiCo_2O_4$ powder, (d) the pore size distribution of $NiCo_2O_4$ powder

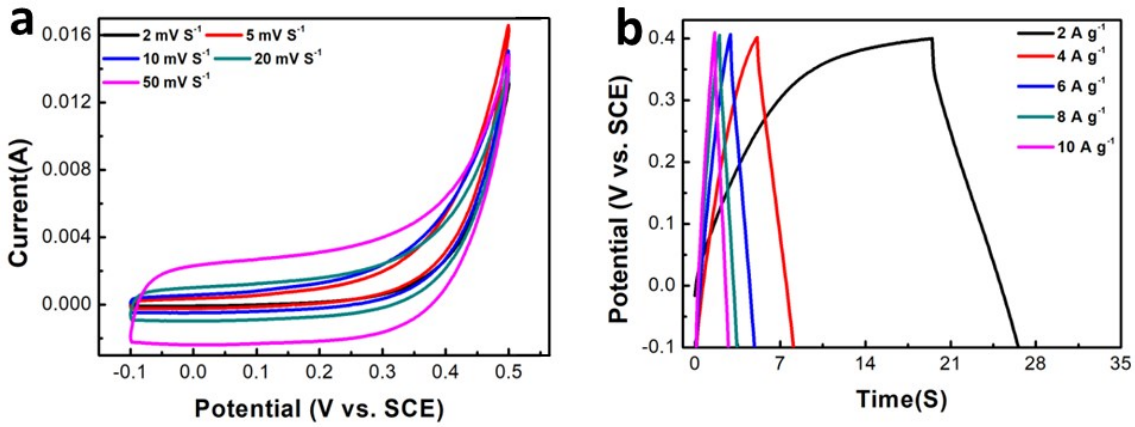

Fig. S13 The electrochemical performance of NSCS: a (CV) and b (GCD) are in 6 M KOH within a potential window of -0.1-0.5 V, the specific capacitance was 24.9 F g^{-1}, 23.7 F g^{-1} at current density of 2 A g^{-1}, 10 A g^{-1}, respectively.

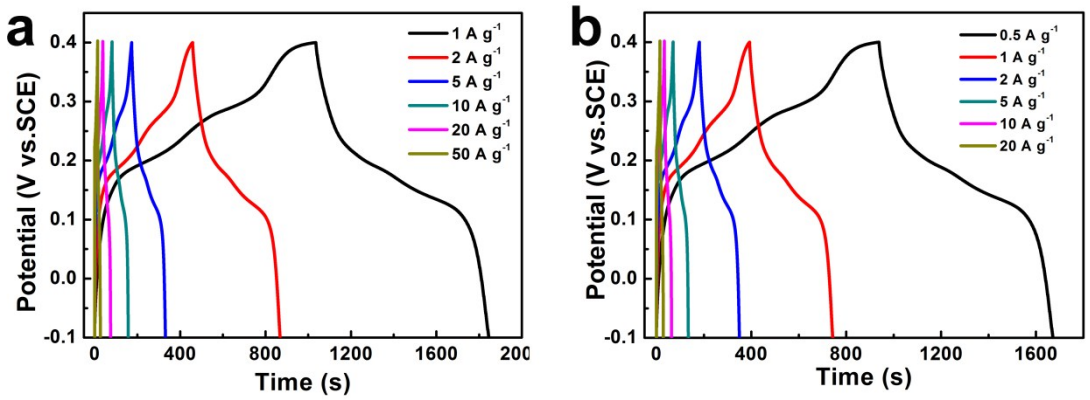

Fig. S14 GCD curves of $NiCo_2O_4$/NSCS with a density of 0.54 g cm^{-3}: (a) Based on the active material; (b) Based on the total mass of whole electrode.

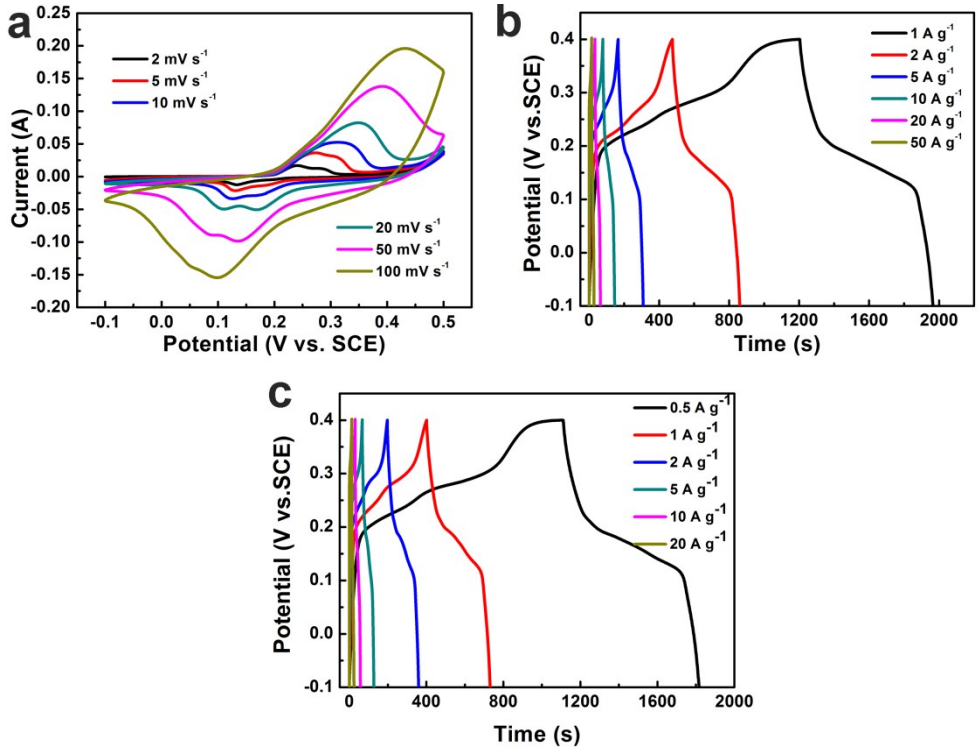

Fig. S15 (a) CV curves , (b) GCD curves (based on the mass of active material) and (c) GCD curves (based on the total mass of whole electrode) of $NiCo_2O_4$/NSCS with a density of 0.92 g cm^{-3}.

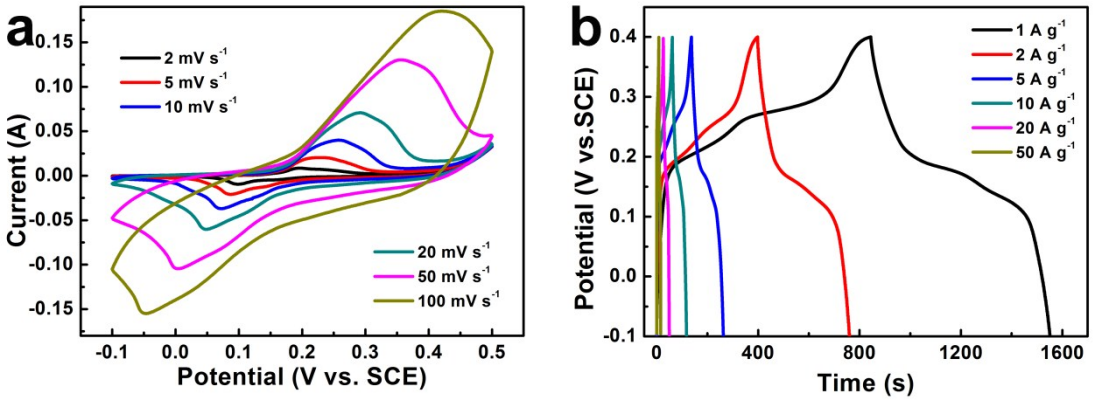

Fig. S16 (a) CV curves and (b) GCD curves (based on the mass of active material) of $NiCo_2O_4$/NSCS with a density of 1.22 g cm^{-3}.

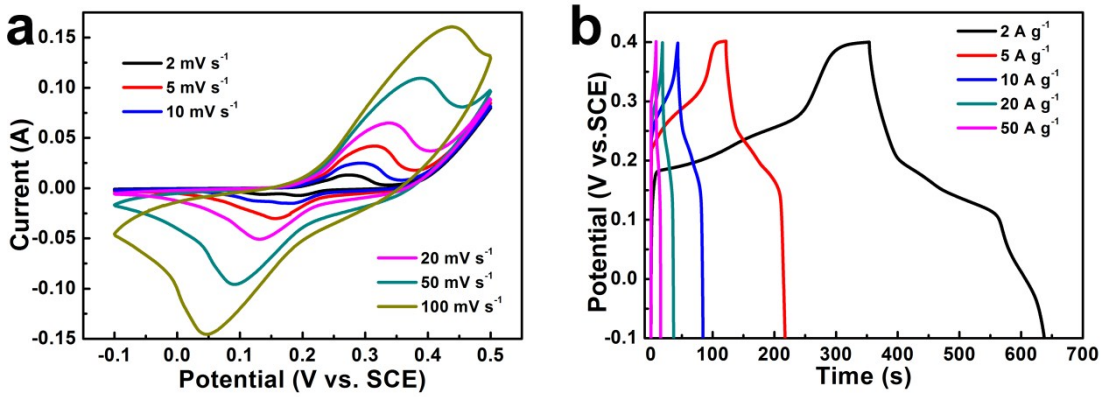

Fig. S17 (a) CV curves and (b) GCD curves (based on the mass of active material) of $NiCo_2O_4$/NSCS with a density of 1.43 g cm^{-3}.

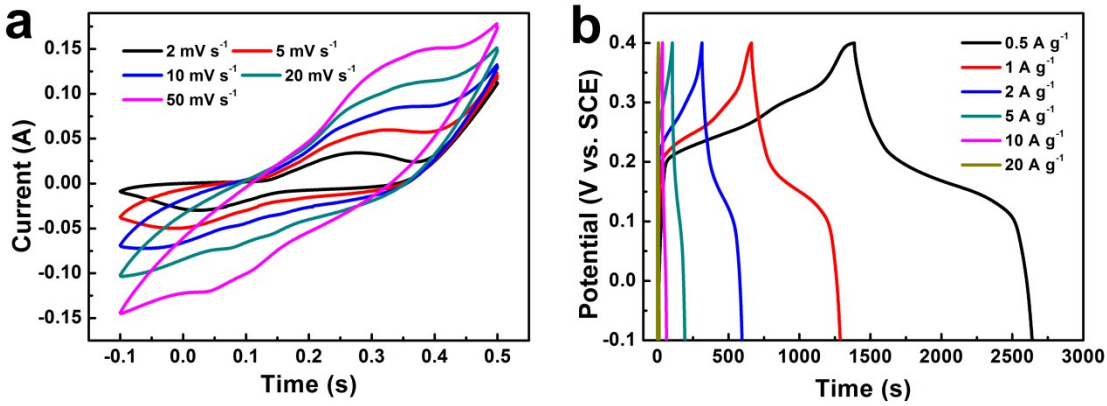

Fig. S18 (a) CV and (b) GCD curves of $NiCo_2O_4$ powder.

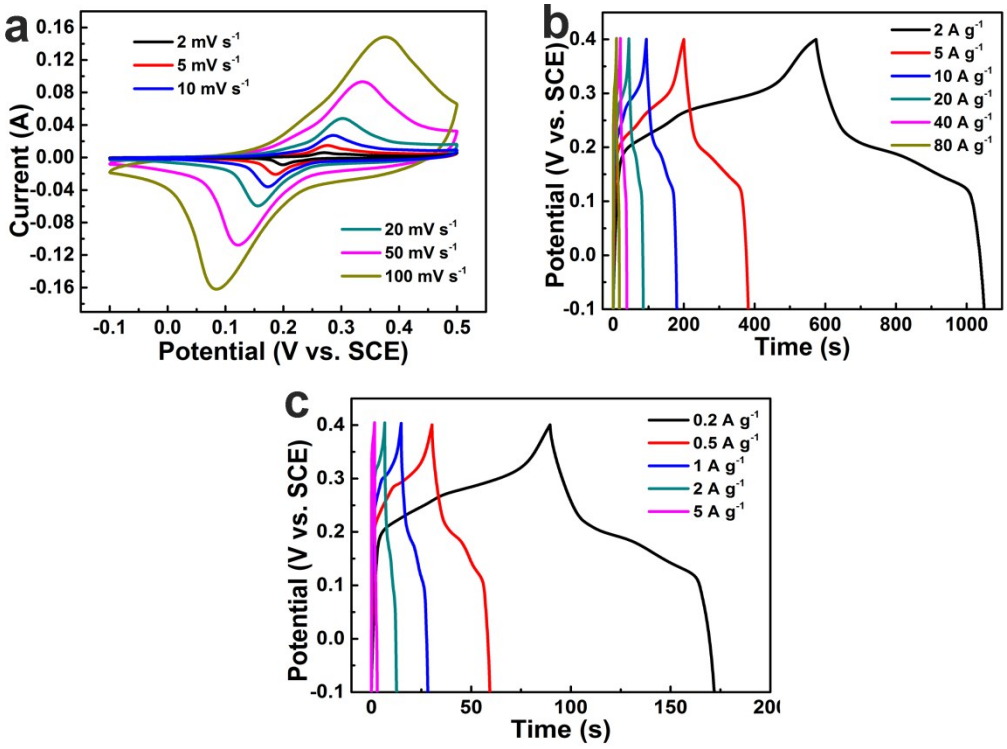

Fig. S19 (a) CV curves , (b) GCD curves (based on the mass of active material) and (c) GCD curves o (based on the total mass of all material) of $NiCo_2O_4$/Ni Foam.

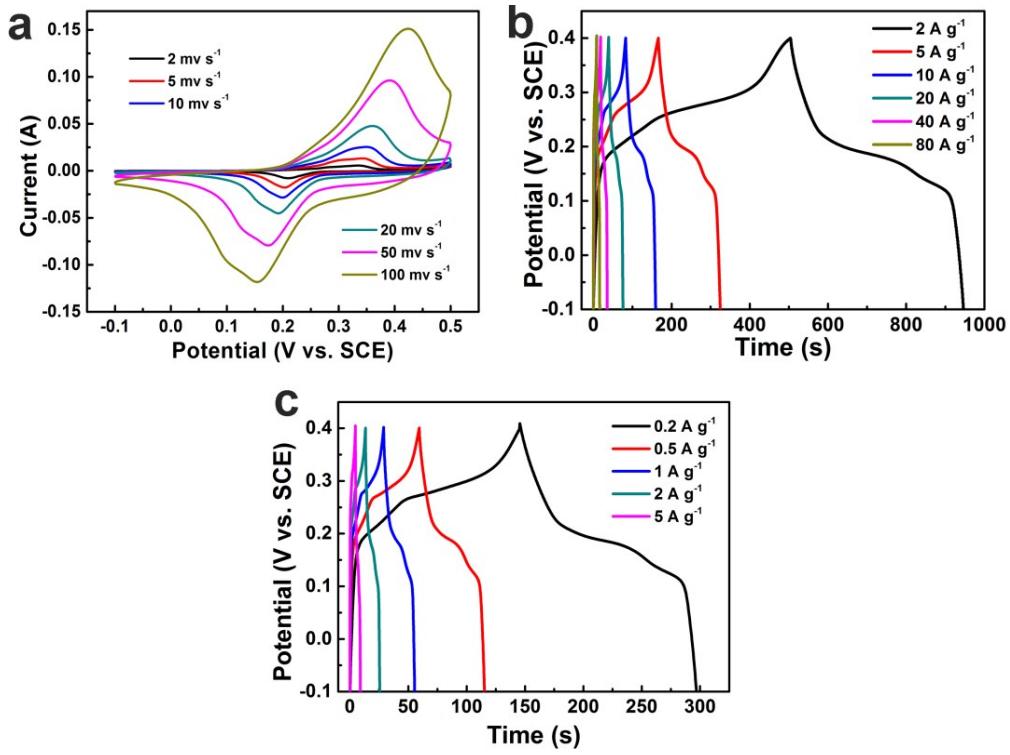

Fig. S20 (a) CV curves , (b) GCD curves (based on the mass of active material) and (c) GCD curves o (based on the total mass of all material) of $NiCo_2O_4$/Carbon Cloth.

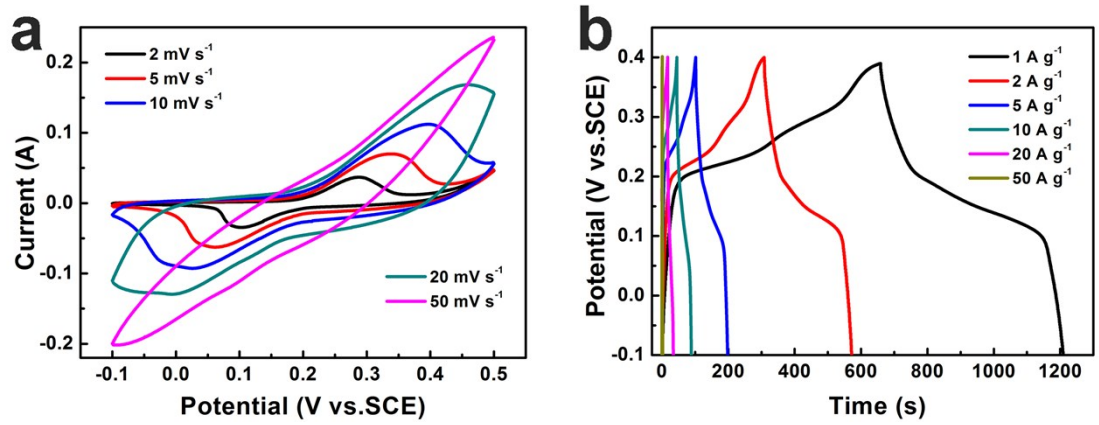

Fig. S21 (a) CV and (b) GCD curves of $NiCo_2O_4$/NSCS with a 72 um thickness in a density of 1.21 g cm^{-3}.

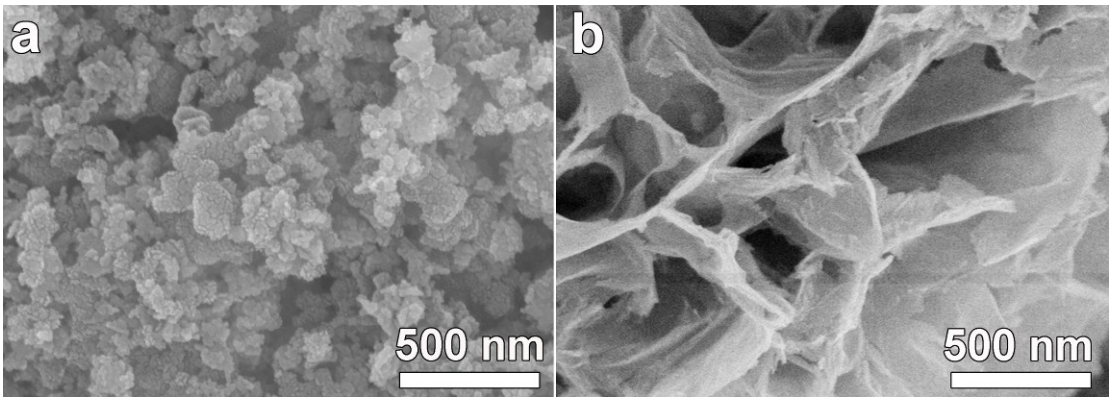

Fig. S22 SEM images after 5000 cycles: (a) $NiCo_2O_4$ powder and (b)$NiCo_2O_4$/NSCS.

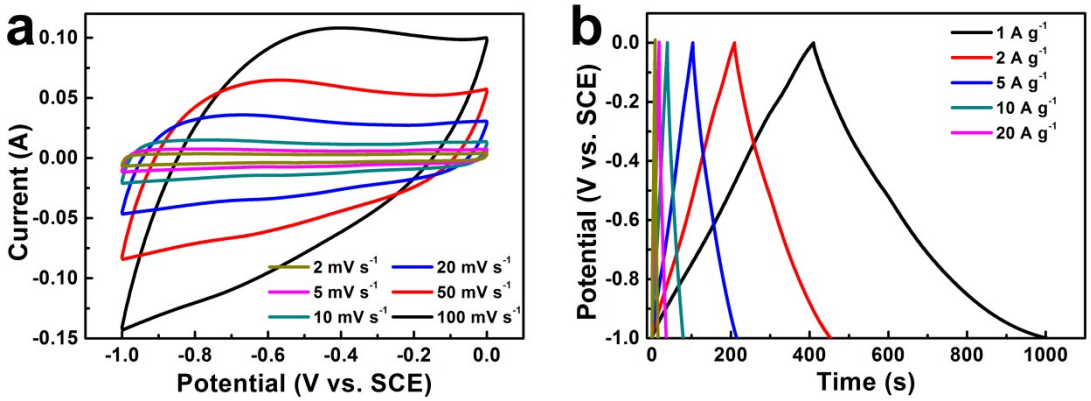

Fig. S23 (a) CV and (b) GCD curves of NGN/CNTs film.

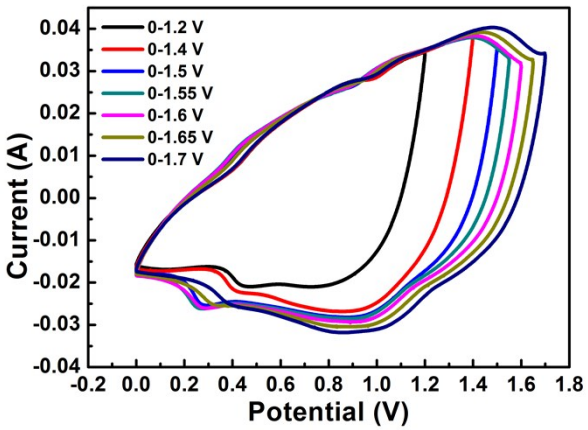

Fig. S24 The CV curves of our ASC at different potential windows (at 50 mV s^{-1})

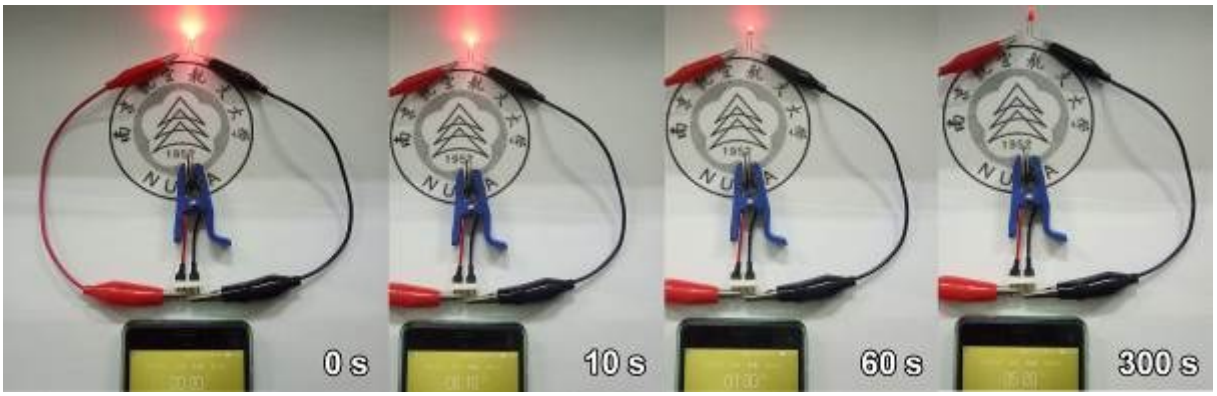

Fig. S25 Images of the red LED driven by two ASCs in series at different stages.

Table S1. Comparision of our work with recently reported high volumetric capacitances of pseudocapacitive materials.

Ref.	Type of materials	Density	Current density (Scan rate)	Gravimetric capacitance	Volumetric capacitance	Rate capability
This work	$NiCo_2O_4$/NSCS	1.43 g cm^{-3}	2 A g^{-1}	1100 F g^{-1}	790 F cm^{-3}	51% (2 to 50 A g^{-1})
This work	$NiCo_2O_4$/ NSCS	1.22 g cm^{-3}	1 A g^{-1}	1414.2 F g^{-1}	785.7 F cm^{-3}	52.3% (1 to 50 A g^{-1})
This work	$NiCo_2O_4$/ NSCS	0.92 g cm^{-3}	1 A g^{-1}	1540.2 F g^{-1}	641.8 F cm^{-3}	64.5% (1 to 50 A g^{-1})
This work	$NiCo_2O_4$/ NSCS	0.54 g cm^{-3}	1 A g^{-1}	1618 F g^{-1}	394.6 F cm^{-3}	72.9% (1 to 50 A g^{-1})
2	$NiCo_2O_4$/Ni Fiber	--	2.5 mA	336 F g^{-1}	29.7 F cm^{-3}	95.5% (2.5 to 20 mA)
3	Network-like mesoporous $NiCo_2O_4$/carbon cloth	--	1 A g^{-1}	1843.3 F g^{-1}	33.75 F cm^{-3}	80% (1 to 32 A g^{-1})
4	Ni–Co hydroxide /graphene petal foam	0.605 g cm^{-3}	5 mA cm^{-2}	--	765 F cm^{-3}	16% (5 to 100 mA cm^{-2})
5	$Ni(OH)_2$/graphene sheet	1.14 g cm^{-3}	0.2 A g^{-1}	573 F g^{-1}	655 cm^{-3}	72% (0.2 to)
6	Ni-Mn oxy-hydroxide@NPM	--	0.5 A cm^{-3}	--	505 cm^{-3}	67% (0.5-10 A cm^{-3})
7	PANI/graphene composite	1.5 g cm^{-3}	0.1 A g^{-1}	546 F g^{-1}	600 F cm^{-3}	66% (0.1 to 10 A g^{-1})
8	MoS_2 nanosheet	2.5 g cm^{-3}	1 mV s^{-1}	280 F g^{-1}	700 F cm^{-3}	--
9	MnO_2/aMEGO	2.5 g cm^{-3}	0.25 A g^{-1}	256 F g^{-1}	640 F cm^{-3}	73% (0.25 to 20 A g^{-1})
10	$Ti_3C_2T_x$ clay	3.67 g cm^{-3}	2 mV s^{-1}	245 F g^{-1}	900 F cm^{-3}	~83% (2 to 100 mV s^{-1})
11	Graphene-MnO_2	1.04 g cm^{-3}	0.5 A g^{-1}	470 F g^{-1}	366 F cm^{-3}	60% (0.5 to 50 A g^{-1})
12	$Ti_3C_2T_x$ /PDDA	3.17 g cm^{-3}	2 mV s^{-1}	167.2 F g^{-1}	530 F cm^{-3}	56.6% (2 to 100 mV

						s^{-1})
13	m-WO_{3-x}/Carbon Nanocomposites	3.3 g cm^{-3}	1 mV s^{-1}	103 F g^{-1}	340 F cm^{-3}	--
14	MoO_{3-x} nanobelt/CNTs	1.33 g cm^{-3}	0.5 A g^{-1}	337 F g^{-1}	291 F cm^{-3}	63.6% (0.5-10 A g^{-1})
15	Graphene foam/MnO_2	0.582 g cm^{-3}	1 A g^{-1}	395 F g^{-1}	230 F cm^{-3}	--
16	MXene/RGO	3.0 g cm^{-3}	2 mV s^{-1}	145 F g^{-1}	435 F cm^{-3}	74% (2 to 200 mV s^{-1})

Table S2. Comparison of electrochemical performance of repoted state-of-the-art ASCs (All normalized to active material).

Ref.	Type of SCs	C_g,	C_v	E_{gmax}	E_{vmax}
This work	$NiCo_2O_4$/NSCS s// NGN/CNTs	134 F g^{-1} (5 mV s^{-1})	94.04 F cm^{-3}	47.65 W h kg^{-1} (536 W kg^{-1})	33.44 W h L^{-1} (376.16 W L^{-1})
17	$NiCo_2O_4$/NGN/CNTs // NGN/CNTs	128 F g^{-1} (1A g^{-1})	77.6 F cm^{-3}	42.71 W h kg^{-1} (775 W kg^{-1})	25.90 W h L^{-1} (469.9 W L^{-1})
18	$NiCo_2O_4$/graphene// HFAC	113 F g^{-1} (0.5 A g^{-1})	--	48 W h kg^{-1} (250 W kg^{-1})	76.3 W h L^{-1}
5	GNiF//GTF	44.8 F g^{-1} (1 A g^{-1})	58.5 F cm^{-3}	18 W h kg^{-1} (850 W kg^{-1})	23.5 W h L^{-1}
19	$Ni(OH)_2$/UGF//a-MEGO	119 F g^{-1} (1 A g^{-1})	--	13.4W h kg^{-1}	8.7 W h L^{-1}
20	$NiCo_2S_4$ NS/NCF// OMC/NCF	128 F g^{-1} (5 mV s^{-1})		45.5 W h kg^{-1} (512 W kg^{-1})	--
21	CNT@$NiCo_2O_4$//AC	91 F g^{-1} (0.5A g^{-1})	--	19.7 Wh kg^{-1} (62.5 W kg^{-1})	--
22	$NiCo_2O_4$@MnO_2// AC	120.9 F g^{-1} (0.25 A g^{-1})		37.8 W h kg^{-1} 187.5 W kg^{-1}	--
23	$NiCo_2O_4$@NiO//AC	73.1 F g^{-1} (1 A g^{-1})		31.5 W h kg^{-1} 215.2 W kg^{-1}	--
24	Ni-Co oxide//AC	288 F g^{-1} (0.5 A g^{-1})		19.5 W h kg^{-1} 150 W kg^{-1}	--
25	AC//CQDs/$NiCo_2O_4$	88.9 F g^{-1} (0.5 A g^{-1})	--	27.8 W h kg^{-1} (128 W kg^{-1})	--
26	$NiCo_2S_4$//G/CS	119.1 F g^{-1} (5 mV s^{-1})	--	42.3 W h kg^{-1} 476 W kg^{-1}	--

Reference

1. W. Bai, H. Tong, Z. Gao, S. Yue, S. Xing, S. Dong, L. Shen, J. He, X. Zhang and Y. Liang, *J. Mater. Chem. A*, 2015, **3**, 21891-21898.
2. A. Ramadoss, K. N. Kang, H.-J. Ahn, S. I. Kim, S. T. Ryu and J.-H. Jang, *J. Mater. Chem. A*, 2016, **4**, 4718-4727.
3. S. Gao, F. Liao, S. Ma, L. Zhu and M. Shao, *J. Mater. Chem. A*, 2015, **3**, 16520-16527.
4. G. Xiong, P. He, D. Wang, Q. Zhang, T. Chen and T. S. Fisher, *Adv. Funct. Mater.*, 2016, **26**, 5460-5470.
5. M. Li, Z. Tang, M. Leng and J. Xue, *Adv. Funct. Mater.*, 2014, **24**, 7495-7502.
6. J. Kang, A. Hirata, H. J. Qiu, L. Chen, X. Ge, T. Fujita and M. Chen, *Adv Mater*, 2014, **26**, 269-272.
7. Y. Xu, Y. Tao, X. Zheng, H. Ma, J. Luo, F. Kang and Q. H. Yang, *Adv. Mater.*, 2016, **27**, 8082-8087.
8. M. Acerce, D. Voiry and M. Chhowalla, *Nat. Nanotechnol.*, 2015, **10**, 313.
9. X. Zhao, L. Zhang, S. Murali, M. D. Stoller, Q. Zhang, Y. Zhu and R. S. Ruoff, *ACS Nano*, 2012, **6**, 5404-5412.
10. M. Ghidiu, M. R. Lukatskaya, M. Q. Zhao, Y. Gogotsi and M. W. Barsoum, *Nature*, 2014, **516**, 78-81.
11. L. Sheng, L. Jiang, T. Wei and Z. Fan, *Small*, 2016, **12**, 5217-5227.
12. Z. Ling, C. E. Ren, M. Q. Zhao, J. Yang, J. M. Giammarco, J. Qiu, M. W. Barsoum and Y. Gogotsi, *PNAS*, 2014, **111**, 16676-16681.
13. C. Jo, J. Hwang, H. Song, A. H. Dao, Y.-T. Kim, S. H. Lee, S. W. Hong, S. Yoon and J. Lee, *Adv. Funct. Mater.*, 2013, **23**, 3747-3754.
14. X. Xiao, Z. Peng, C. Chen, C. Zhang, M. Beidaghi, Z. Yang, N. Wu, Y. Huang, L. Miao, Y. Gogotsi and J. Zhou, *Nano Energy*, 2014, **9**, 355-363.
15. L. Zhang, D. DeArmond, N. T. Alvarez, D. Zhao, T. Wang, G. Hou, R. Malik, W. R. Heineman and V. Shanov, *J. Mater. Chem. A*, 2016, **4**, 1876-1886.
16. M. Q. Zhao, C. E. Ren, Z. Ling, M. R. Lukatskaya, C. Zhang, K. L. Van Aken, M. W. Barsoum and Y. Gogotsi, *Adv. Mater.*, 2015, **27**, 339-345.
17. S. Yue, H. Tong, L. Lu, W. Tang, W. Bai, F. Jin, Q. Han, J. He, J. Liu and X. Zhang, *J. Mater. Chem. A*, 2017, **5**, 689-698.
18. Z. Li, Z. Xu, H. Wang, J. Ding, B. Zahiri, C. M. B. Holt, X. Tan and D. Mitlin, *Energy Environ. Sci.*, 2014, **7**, 1708-1718.
19. J. Ji, L. L. Zhang, H. Ji, Y. Li, X. Zhao, X. Bai, X. Fan, F. Zhang and R. S. Ruoff, *ACS Nano*, 2013, **7**, 6237-6243.
20. L. Shen, J. Wang, G. Xu, H. Li, H. Dou and X. Zhang, *Adv. Energy Mater.*, 2015, **5**, 1400977.
21. F. Cai, Y. Kang, H. Chen, M. Chen and Q. Li, *J. Mater. Chem. A*, 2014, **2**, 11509-11515.
22. Y. Zhang, B. Wang, F. Liu, J. Cheng, X.-w. Zhang and L. Zhang, *Nano Energy*, 2016, **27**, 627-637.
23. X. J. Liu, J. F. Liu and X. M. Sun, *J. Mater. Chem. A*, 2015, **3**, 13900-13905.
24. H. Wang, C. M. B. Holt, Z. Li, X. Tan, B. S. Amirkhiz, Z. Xu, B. C. Olsen, T. Stephenson and D. Mitlin, *Nano Res.*, 2012, **5**, 605-617.
25. Y. Zhu, Z. Wu, M. Jing, H. Hou, Y. Yang, Y. Zhang, X. Yang, W. Song, X. Jia and X. Ji, *J. Mater. Chem. A*, 2014, **3**, 866-877.

26. L. Shen, L. Yu, H. B. Wu, X. Y. Yu, X. Zhang and X. W. Lou, *Nat. Commun.*, 2015, **6**, 6694.